

# Propagating Measurement Uncertainty to Microwave Amplifier Nonlinear Behavioral Models

Laurence T. Stant<sup>1</sup>, *Student Member, IEEE*, Martin J. Salter, *Member, IEEE*, Nick M. Ridler<sup>2</sup>, *Fellow, IEEE*, Dylan F. Williams<sup>3</sup>, *Fellow, IEEE*, and Peter H. Aaen, *Senior Member, IEEE*

**Abstract**—We propagate for the first time correlated measurement uncertainties into a nonlinear behavioral model of a millimeter-wave amplifier. We make use of the National Institute of Standards and Technology Microwave Uncertainty Framework to evaluate the uncertainties in large-signal electromagnetic wave measurements of an amplifier, followed by the extraction of  $X$ -parameters using an industry standard algorithm. This extracted model is included as a component in a circuit simulator to evaluate gain and efficiency incorporating measurement uncertainty.

**Index Terms**—Measurement uncertainty, microwave amplifiers, microwave measurement, millimeter wave measurements, millimeter wave transistors, parameter extraction, power amplifiers.

## I. INTRODUCTION

THE increasing demands for bandwidth and power efficiency in 5G wireless communications are placing more focus on accurate characterization and linearization of nonlinear radio frequency, microwave, and millimeter-wave amplifiers. To extract models from these devices requires measurement, and it is well known that all physical measurements incorporate uncertainty caused by systematic (nonvarying) and random errors. Because device models are central to modern amplifier design, accurate development is crucial to ensure first-pass design success. Therefore, the availability of information about measurement uncertainty, and the ability to propagate this through the device model into end-user circuit designs, is very valuable when both developing a device model and later evaluating circuit performance [1].

The characterization of linear devices is often performed using a vector network analyzer (VNA) [2].

Manuscript received April 20, 2018; revised August 26, 2018; accepted September 28, 2018. Date of publication November 30, 2018; date of current version February 5, 2019. This work was supported through an Engineering and Physical Sciences Research Council Strategic Equipment Grant EP/L02263X/1. (*Corresponding author: Laurence T. Stant.*)

L. T. Stant and P. H. Aaen are with the Department of Electrical and Electronic Engineering, University of Surrey, Guildford GU2 7XH, U.K., and also with the National Physical Laboratory, Teddington TW11 0LW, U.K. (e-mail: l.stant@surrey.ac.uk).

M. J. Salter and N. M. Ridler are with the National Physical Laboratory, Teddington TW11 0LW, U.K.

D. F. Williams is with the National Institute of Standards and Technology, Boulder, CO 80305 USA.

Color versions of one or more of the figures in this paper are available online at <http://ieeexplore.ieee.org>.

Digital Object Identifier 10.1109/TMTT.2018.2881087

This instrument measures electromagnetic scattering parameters (S-parameters), which completely define the response of a linear device. Through calibration processes, systematic errors in VNA measurements can be significantly reduced, and there has been much study of the residual uncertainty that remains due to imperfect calibration and random errors [3]–[7]. The evaluation of this uncertainty is typically referenced to national measurement standards through a traceability chain [8], and there are guidelines available for evaluations which are compatible with industry requirements [9], [10].

In the nonlinear operating regime, S-parameters no longer capture the complete amplifier response, and a large-signal network analyzer (LSNA) is instead used to measure electromagnetic waves interacting with the device-under-test (DUT) [11], [12]. The evaluation of uncertainties in LSNA measurements must consider additional systematic and random errors contributed by absolute phase and power calibrations, when compared with evaluations of VNA measurements [13]. The first complete evaluation of uncertainty in LSNA measured wave parameters [14] used analytical covariance techniques, followed by numerical solutions in [15] which then propagated the uncertainties into a compact device model. This paper was also the first to use a fully traceable comb generator phase reference, characterised using the electrooptic sampling system at the National Institute of Standards and Technology (NIST). In addition, NIST provides a readily available software microwave uncertainty framework (MUF) [16] which includes the LSNA uncertainty evaluation used in [15]. This software performs an LSNA calibration which propagates uncertainty from both the measurements and definitions of the calibration standards and the measurements of the DUT. The outputs of the framework are calibrated electromagnetic wave measurements of the DUT.

In order to characterize a nonlinear device over a useful operating range, significantly more measurement data are required than for linear devices. Typical measurements include sweeps of fundamental frequency and source power, and also the port, frequencies, and phases of various small-signal tones incident on the device in order to characterize the response to different impedances at each harmonic. To reduce the requirement for long measurement times and large file sizes, the device behavior can be approximated by a nonlinear behavioral model (NLBM). Popular implementations of these

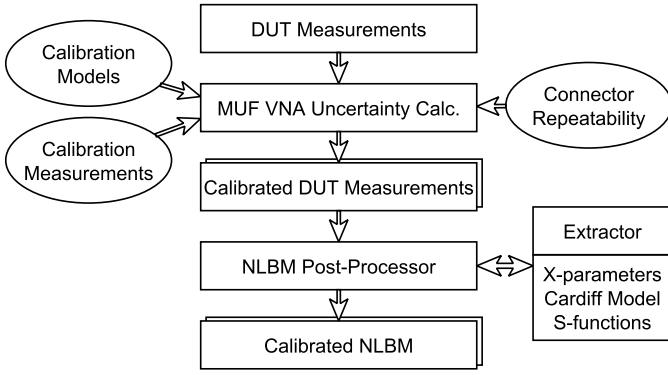


Fig. 1. Processing flow required for a typical evaluation of measurement uncertainty in a NLBM using the NIST MUF.

models include  $X$ -parameters [17],  $S$ -functions [18], and the Cardiff model [19]. To date, although there has been initial work concerning compact models [1], [15], there is no published work showing measurement uncertainty evaluated for a NLBM.

In this paper, we demonstrate for the first time, the evaluation of LSNA measurement uncertainties and their propagation into a NLBM, specifically  $X$ -parameters. Our approach, as illustrated in Fig. 1, uses the NIST MUF to obtain traceable uncertainties in electromagnetic wave parameters, followed by the LSNA  $X$ -parameter extraction routine. By using the LSNA to perform the  $X$ -parameter extraction, we ensure the extracted model definition is identical to that used in industry (although other extraction algorithms can be used). Once the model has been extracted including measurement uncertainty, it can be used within a circuit simulator to perform a Monte Carlo analysis of the complete circuit performance.

The paper is organized as follows: Section II describes the  $X$ -parameters and the measurement procedure required for extraction. Section III describes the nonlinear calibration and measurements of large-signal electromagnetic waves of a millimeter-wave amplifier with uncertainties. Section IV presents the approach used to extract the  $X$ -parameter NLBM with uncertainties. Section V presents the results obtained, including a sensitivity analysis of the  $X$ -parameters to identify significant sources of uncertainty. Section VI discusses the use of the extracted uncertain  $X$ -parameter model in circuit simulators and gives an example.

## II. $X$ -PARAMETER BEHAVIORAL MODEL

$X$ -parameters [17] are a superset of linear scattering parameters, which can be shown to relate the scattered wave  $B_{p,k}$  to the incident wave  $A_{q,l}$  through

$$B_{p,k} = X_{p,k}^F(|A_{1,1}|)P^k + \sum_{q,l \neq (1,1)} [X_{p,k;q,l}^S(|A_{1,1}|)A_{q,l}P^{k-l} + X_{p,k;q,l}^T(|A_{1,1}|)A_{q,l}^*P^{k+l}] \quad (1)$$

$$P = \frac{A_{1,1}}{|A_{1,1}|} = e^{j \cdot \text{phase}(A_{1,1})} \quad (2)$$

where  $A_{1,1}$  is the large-signal stimulus applied at the fundamental frequency at port 1,  $X^F$  are the parameters that define the response at port  $p$  and harmonic  $k$  when the DUT has all ports matched, and  $X^S$  and  $X^T$  are the partial derivatives of the nonanalytic model which determines the response at port  $p$ , harmonic  $k$ , from small-signal reflections (caused by mismatches) incident on port  $q$  at harmonic  $l$  [20].

To extract  $X$ -parameters, electromagnetic waves are measured at several harmonics for large-signal stimuli swept over a range of powers and fundamental frequencies. From these measurements, we can obtain  $X^F$  parameters. To extract the remaining parameters, the small-signal linear response of the DUT at each large-signal stimuli, also called a large signal operating point (LSOP), is then measured. At each LSOP, a second weaker tone, the extraction tone, is applied, in turn, to each port at each harmonic. Measurements are made for a number of phases of each extraction tone, which are typically used in a least-squares regression technique to calculate the small-signal  $X^S$  and  $X^T$  parameters. Behavioral models which use a higher order representation for the small-signal responses can use a similar measurement approach with a larger number of extraction tone phases.

## III. LSNA CALIBRATION WITH UNCERTAINTIES

The NIST MUF was used to perform the calibration of electromagnetic wave parameters measured using a Keysight Technologies 67-GHz N5247A PNA-X LSNA.<sup>1</sup> The DUT was an internally matched Analog Devices HMC342LC4 low noise amplifier [21] mounted on a connectorized evaluation board. This amplifier has a typical gain of 19 dB and a 1-dB compression point at approximately 9-dBm output power at 25 GHz. To obtain results showing both the linear and nonlinear regimes of operation, the source power was swept between  $-22$  and  $-2$  dBm in 0.25-dB steps. The fundamental frequency was set at 25 GHz with a harmonic at 50 GHz also measured. The evaluation board used 2.92-mm precision connectors, connected via adapters to cables with 2.4-mm precision connectors. The calibration plane was located between the cables and the adapters (i.e., the adapters were included as part of the DUT), and the measurement setup had a nominal impedance of 50  $\Omega$ . The intermediate frequency bandwidth was set to 10 Hz. The built-in  $X$ -parameter measurement routine was used and configured to extract cross-frequency terms between both harmonics using measurements at four extraction tone phases (this is the default setting). A photograph of the setup is shown in Fig. 2.

LSNA calibration consists of two steps. First, an eight-term calibration is performed using any algorithm compatible with linear VNA calibration, e.g., one could use a short-open-load-thru or thru-reflect-line (TRL) algorithm and measure appropriate calibration standards. The second step is to perform an absolute calibration, which uses measurements of a harmonic phase reference and a power meter to replace the normalized transmission term in the eight-term error model determined by the first step.

<sup>1</sup>We use brand names to more completely describe our experiment. NPL/NIST do not endorse commercial products. Other products may perform as well or better.

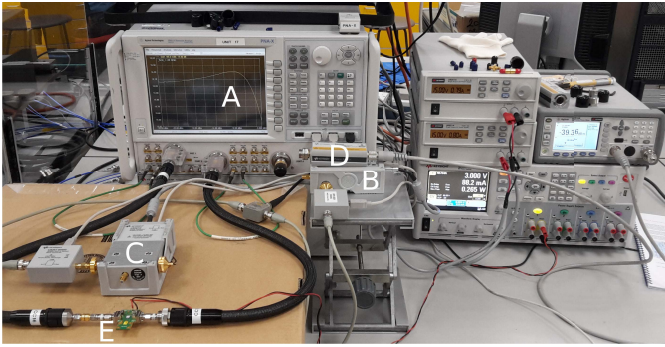


Fig. 2. Measurement setup used for extracting  $X$ -parameters from the DUT. (A) PNA-X LSNA, (B) phase reference comb generator, (C) phase calibration comb generator, (D) power meter, and (E) connected DUT.

Uncertainties are propagated through all steps of the calibration by the MUF. We have included uncertainties present in the definitions and measurements of the passive calibration standards, the power meter calibration and measurement, the phase reference characterization and measurement, cable flexure, and connection repeatability of all calibration steps. Uncertainty due to random noise in the high-dynamic range receivers was omitted as it has been shown to be negligible with respect to that arising from other error sources in LSNA measurements [13].

The MUF provides two methods which propagate uncertainty through the calibration. The first uses a Monte Carlo analysis [22] to simultaneously perturb each input quantity by a random amount subject to its assigned distribution, then performs the calibration to obtain a set of results. This process is repeated many times to build a collection of results. Statistical analysis is then performed on these results to determine their standard uncertainties. This propagation method preserves nonlinearities in the calibration but may require long processing times if a large amount of results are required or the calibration is computationally intensive.

The second method is a linear propagation of uncertainty in the form of a sequential perturbation analysis [23, Sec. 5.1.4]. Each error source, in turn, is perturbed by its standard uncertainty and all other sources held at their estimated value. The deviations from the estimate of the result can then be combined (using root sum of squares) to produce a combined standard uncertainty in the result. Each result from the sequential perturbation can then be compared with this value, providing a sensitivity analysis of the result to each error source. Because the number of input quantities is typically much smaller than the suitable number Monte Carlo simulations, this method can be much faster than the Monte Carlo propagation but uses a linear approximation of the calibration. This is generally a valid approximation if the uncertainties in the error sources are small.

The MUF supports several calibration algorithms, and for this measurement the multiline TRL calibration algorithm [24], [25] was chosen to allow direct dimensional traceability to national measurement standards. The calibration standards used were from a 1.85-mm precision coaxial calibration kit (Rosenberger RPC-1.85 LRL). Table I gives the dimensions

TABLE I  
NOMINAL VALUES AND STANDARD UNCERTAINTIES  
FOR THE TRL COAXIAL LINE STANDARDS

| Dimension         | Line 1 value (mm)  | Line 2 value (mm)  |
|-------------------|--------------------|--------------------|
| Line length       | $13.004 \pm 0.003$ | $14.913 \pm 0.003$ |
| Line inside dia.  | $0.803 \pm 0.001$  | $0.803 \pm 0.008$  |
| Line outside dia. | $1.850 \pm 0.005$  | $1.850 \pm 0.005$  |

TABLE II  
STANDARD UNCERTAINTIES FOR POWER METER UNCERTAINTY  
CONTRIBUTIONS DERIVED IN [26]

| Contribution                           | Standard uncertainty  |
|--|-----------------------|
| Reference oscillator mismatch          | 0.2%                  |
| Reference oscillator power uncertainty | 0.6%                  |
| Zero-set error                         | 0.5% meter full scale |
| Zero carry-over error                  | 0.2% meter full scale |
| Instrumentation error                  | 0.5% meter full scale |
| Calibration factor error               | 0.024                 |

of the line standards used for the calibration. To include the effect of connector repeatability on the passive calibration, each standard was measured several times with the connector oriented differently. These measurements were passed to a MUF program (“Combine”) which produces a mean value with an associated uncertainty.

The power meter measurement, as part of the absolute calibration, measures the amplitude of the waves. The calibration model for the power meter itself is defined in [26] and includes the reference oscillator mismatch, the reference oscillator power uncertainty, the zero-set error, the zero carry-over error, the instrumentation error, and error in the power sensor calibration factor. The estimates and uncertainties used for these parameters in the calibration are given in Table II and are derived from specifications supplied by the manufacturer. The mismatch of the power sensor was also measured using a calibrated VNA and included in the absolute calibration. Connector repeatability was assessed for this measurement in the same way as for the passive standards.

In order to complete the absolute calibration, the phase must also be calibrated. This is performed using a harmonic phase reference, which for this calibration was provided by a Keysight Technologies 67-GHz comb generator [27]. This device supplies a stable and repeatable train of pulses, which creates a frequency comb (aligned to the calibration frequencies) to be measured by the LSNA. The phase uncertainties are given in Table III and were obtained through characterization with a sampling oscilloscope at NIST, which is traceable to national measurement standards via electrooptic calibration [28], [29].

#### IV. PROPAGATION OF UNCERTAINTY TO $X$ -PARAMETERS

Once the corrected, correlated large-signal wave measurements, and uncertainties have been obtained from the MUF, we extracted the  $X$ -parameter model. We have implemented this routine as a postprocessor within the MUF which makes use of the PNA-X “NVNA” software. We provide the software

TABLE III  
NOMINAL PHASE AND STANDARD UNCERTAINTY FOR HARMONIC  
PHASE REFERENCE AT CALIBRATION FREQUENCIES

| Frequency (GHz) | Characterized phase (deg.) | Measured phase (deg.) |
|-----------------|----------------------------|-----------------------|
| 25              | $181.5 \pm 0.4$            | $-16.8 \pm 1.5$       |
| 50              | $170.8 \pm 1.0$            | $61.0 \pm 2.5$        |

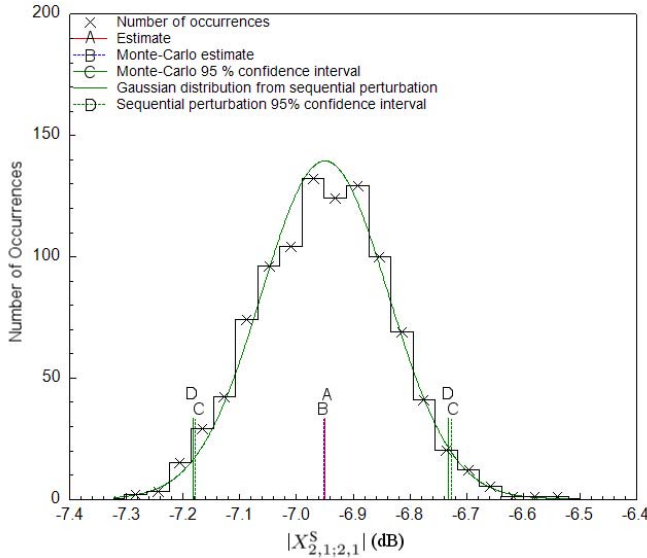


Fig. 3. Histogram comparing the Monte Carlo and sequential perturbation uncertainty results for  $X_{2,1;2,1}^S$  (25 GHz) of the DUT at  $-2.4$ -dBm source power. The vertical line in the center of the plot (A) shows the nominal value (estimate), (B) shows the Monte Carlo average, and (C) and (D) show the Monte Carlo and sequential perturbation 95% confidence intervals, respectively.

with corrected wave files with added swept variables which relate to the Monte Carlo and sensitivity analysis sample indices produced by the MUF.

The MUF preserves all correlations in the input quantities, including those between wave measurements at different frequencies. This information is required if the results are going to be used in models which take cross-frequency data as their inputs. Previously, this has been shown for Fourier transforms [1], [15], but it is also true for some terms in NLBMs (e.g.,  $X_{p,k;q,l}^S$  and  $X_{p,k;q,l}^T$  where  $k \neq l$ ).

## V. EXAMPLE POWER AMPLIFIER MEASUREMENT

### A. X-Parameter Uncertainties

In this example, we used Monte Carlo with 1000 samples to propagate uncertainty to the  $X$ -parameters of the DUT. This required 8 h of processing for the calibration and a further 8 h of processing for the  $X$ -parameter extraction. A histogram is provided in Fig. 3 showing a good agreement between the Monte Carlo and sensitivity analysis. This level of agreement is typical for all of the extracted  $X$ -parameters.

The estimated values and standard uncertainties from the Monte Carlo analysis for the magnitude and phase of a sample of  $X$ -parameter terms are shown in Fig. 4. It can be seen in all plots that there is a clear change in uncertainty for several

$X$ -parameters as the DUT transitions between the linear and nonlinear regimes.

The phase noise seen at lower powers in the estimate of  $X_{2,1;2,2}^T$  is not accompanied by an increase in measurement uncertainty. This suggests that it arises from the extraction routine, which contributes another source of uncertainty not studied in this paper. By design, the  $X^T$  parameters are negligible in the linear regime, and so this effect will have little contribution when the model is used.

### B. Sensitivity Analysis for X-Parameter Uncertainties

Fig. 5 shows a sample of the sensitivity analysis results for the  $X$ -parameter uncertainty obtained using sequential perturbation. Over 300 sources of uncertainty were included in the analysis and they have been grouped for clarity.

It can be seen in Fig. 5(a) that the power calibration has a dominant contribution to the uncertainty in the magnitude of  $X_{12}^F$ . This is to be expected because  $X^F$  terms represent the absolute electromagnetic waves output from the DUT, and the uncertainties from the power meter in the LSNA calibration (i.e., in the corrected wave measurements) are significantly larger than those from the TRL standards.

The TRL calibration uncertainty is also a dominant contribution to the uncertainty in the magnitude of most of the small-signal  $X^S$  and  $X^T$  terms. Because these terms are similar to S-parameters, in that they represent a ratio between electromagnetic waves, any correlated error components are canceled. Both the power and phase calibration errors are correlated for terms concerning a single frequency but only power calibration errors appear to be correlated for cross-frequency terms. This can be seen from the lack of uncertainty contribution from the phase calibration to the  $X_{2,1;2,1}^T$  term.

For our example measurements, it can be seen that the uncertainty contribution from cable flexure (and reconnection) was significant in all results. This is a well-known issue for electromagnetic measurements at millimeter-wave frequencies and above. This uncertainty contribution could be reduced by limiting cable movement.

## VI. USE IN CIRCUIT SIMULATORS

Once the behavioral model has been extracted from measurements, it can be used in circuit simulators to predict the performance of circuit designs. Because the uncertainty information is stored as a collection of samples, it can be propagated through the circuit simulator by sweeping the sample index and running the simulation for each value. From this array of results, a statistical analysis can be performed to determine the standard uncertainty of the performance metric in question. The sensitivity analysis can be propagated in a similar way as there is a sample in the model file for the perturbation of each input quantity. It is also possible to evaluate uncertainty in circuit simulations containing multiple DUTs processed using the MUF, for example, in a two stage, balanced, or Doherty amplifier configuration. If the same variable is used to sweep the sample index for all DUTs, then any uncertainty correlations will be preserved. An example would be if multiple DUTs in the circuit were measured

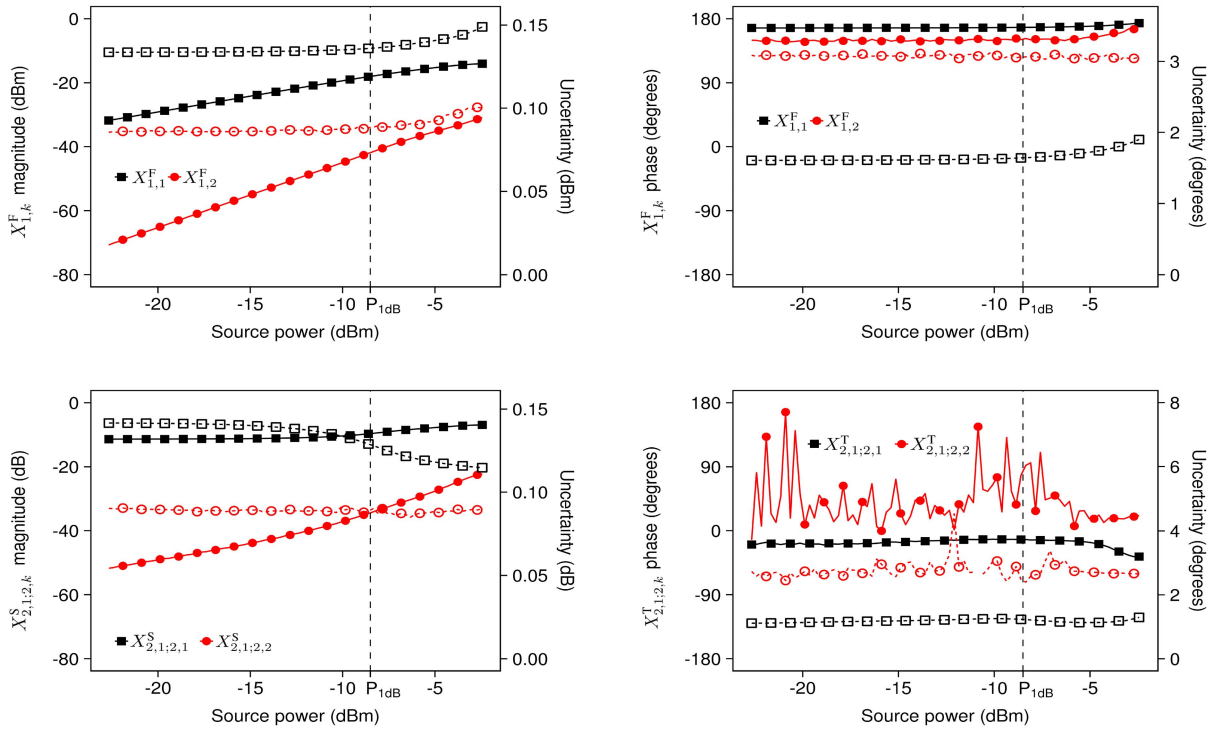


Fig. 4. Estimates (solid line and shapes, left scale) and standard uncertainties (dashed line and hollow shapes, right scale) for the magnitude and phase of a sample of the extracted  $X$ -parameters. Harmonic indices 1 and 2 relate to measurement frequencies of 25 and 50 GHz, respectively. Uncertainties are a linear variation of the scale value.

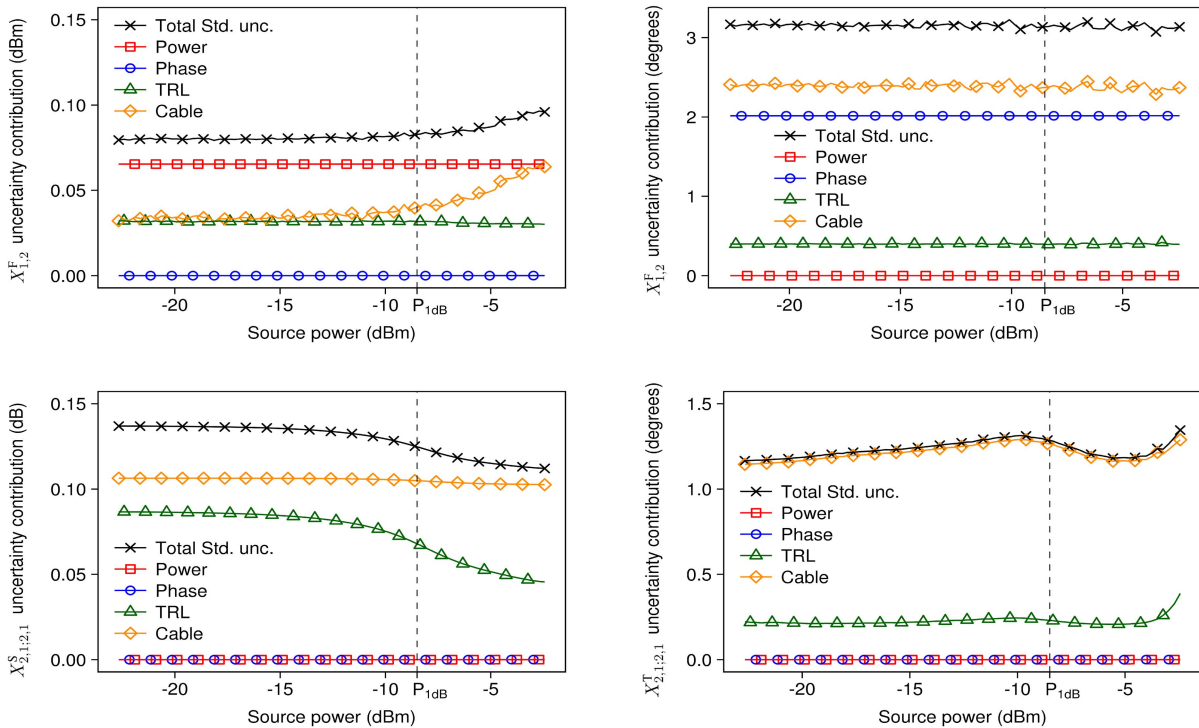


Fig. 5. Sensitivity analysis results for a sample of the extracted  $X$ -parameters. Harmonic indices 1 and 2 relate to measurement frequencies of 25 and 50 GHz, respectively. Because the uncertainty is expressed as a linear variation of a decibel value, a nonzero horizontal line represents a linear relationship with source power.

on an LSNA using the same calibration. The measurement uncertainties that were captured into the  $X$ -parameter behavioral model can now be propagated to typical circuit metrics such as forward gain, input or output match, power-added

efficiency (PAE), error vector magnitude, and adjacent channel power ratio.

To demonstrate this, an example simulation has been created in Advanced Design System (ADS). The DUT is represented

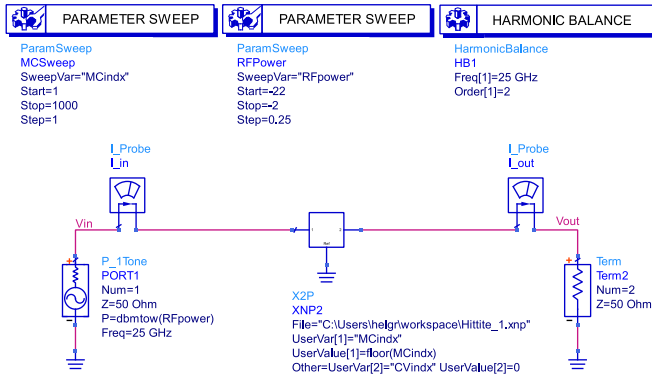


Fig. 6. Example circuit simulation schematic using an X-parameter model in ADS. The source power and X-parameter Monte Carlo sample index is swept by the parameter sweep components, and a harmonic balance simulation is carried out for each value of those sweeps.

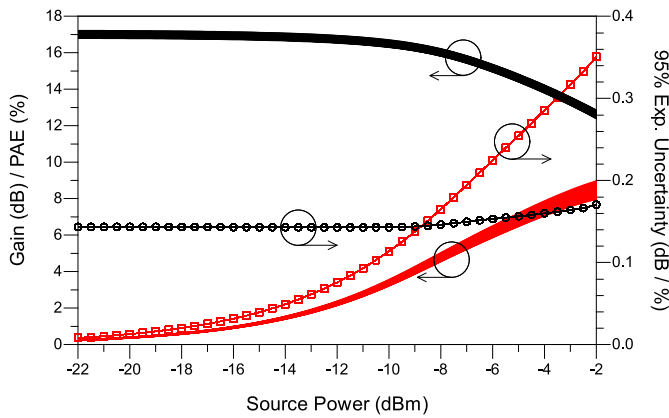


Fig. 7. Results from the ADS circuit simulation. Black higher trace: Monte Carlo samples for the gain of the circuit. Red lower trace: PAE. Black trace with circles and red trace with squares: 95% expanded uncertainties for gain and PAE, respectively.

as an X-parameter model, and the simulator sweeps both the Monte Carlo sample index and the source power using the results from the MUF uncertainty evaluation. For this example, the X-parameter file from the previous section was used. The schematic of the design is shown in Fig. 6, and typical design plots of gain and PAE are provided in Fig. 7. It can be seen that although the uncertainties of both parameters increase significantly with source power, the 95% expanded uncertainties are below 0.2 dB and 0.4% for gain and PAE, respectively.

## VII. CONCLUSION

We have developed a framework to propagate measurement uncertainty to microwave and millimeter-wave amplifier nonlinear behavioral models through Monte Carlo and linear sensitivity analysis approaches. Both approaches preserve correlations between errors and provide a rigorous evaluation. We have demonstrated this by extracting X-parameters with uncertainties from a typical millimeter-wave amplifier. The resulting model has been incorporated into circuit simulations to obtain gain and PAE results incorporating measurement uncertainty. Our example extracted amplifier model exhibited 95% expanded uncertainties of less than 0.2-dB gain and less than 0.4% PAE.

To improve confidence in the design process of systems involving nonlinear devices, the uncertainty in both compact and behavioral models is required. This paper has produced, for the first time, an evaluation of measurement uncertainty in a popular behavioral model by developing a framework which can be easily adapted to support alternative models. In addition, the produced portable device model can be used in existing circuit simulators, allowing access to this information for statistical design techniques and to help achieving first-pass design success for complicated nonlinear systems.

## ACKNOWLEDGMENT

The authors would like to thank G. Avolio and S. Gillespie for helpful discussions during the preparation of this paper, and D. Stokes for assistance with the TRL calibration standards. Publication of the U.S. Government not subject to copyright.

## REFERENCES

- [1] D. F. Williams, R. A. Chamberlin, W. Zhao, J. Cheron, and M. E. Urteaga, "Transistor model verification including measurement uncertainty," *IEEE Trans. Microw. Theory Techn.*, vol. 64, no. 11, pp. 3927–3933, Nov. 2016.
- [2] D. Rytting, "ARFTG 50 year network analyzer history," in *Proc. 71st ARFTG Microw. Meas. Conf.*, Jun. 2008, pp. 1–8.
- [3] A. Lewandowski, D. F. Williams, P. D. Hale, J. C. M. Wang, and A. Dienstfrey, "Covariance-based vector-network-analyzer uncertainty analysis for time- and frequency-domain measurements," *IEEE Trans. Microw. Theory Techn.*, vol. 58, no. 7, pp. 1877–1886, Jul. 2010.
- [4] M. Garelli and A. Ferrero, "A unified theory for S-parameter uncertainty evaluation," *IEEE Trans. Microw. Theory Techn.*, vol. 60, no. 12, pp. 3844–3855, Dec. 2012.
- [5] A. Arsenovic, L. Chen, M. F. Bauwens, H. Li, N. S. Barker, and R. M. Weikle, "An experimental technique for calibration uncertainty analysis," *IEEE Trans. Microw. Theory Techn.*, vol. 61, no. 1, pp. 263–269, Jan. 2013.
- [6] V. Teppati and A. Ferrero, "A comparison of uncertainty evaluation methods for on-wafer S-parameter measurements," *IEEE Trans. Instrum. Meas.*, vol. 63, no. 4, pp. 935–942, Apr. 2014.
- [7] V. Teppati, S. Tirelli, R. Lövlblom, R. Flückiger, M. Alexandrova, and C. R. Bolognesi, "Accuracy of microwave transistor  $f_T$  and  $f_{MAX}$  extractions," *IEEE Trans. Electron Devices*, vol. 61, no. 4, pp. 984–990, Apr. 2014.
- [8] K. Wong, "Traceability of vector network analyzer measurements," in *Proc. 72nd ARFTG Microw. Meas. Symp.*, Portland, OR, USA, Dec. 2008, pp. 157–167.
- [9] *Guidelines on the Evaluation of Vector Network Analysers (VNA)*. EURAMET, Braunschweig, Germany, 2011.
- [10] *General Requirements for the Competence of Testing and Calibration laboratories*, ISO/IEC Standard 17 025:2005, 2005.
- [11] P. Blockley, D. Gunyan, and J. B. Scott, "Mixer-based, vector-corrected, vector signal/network analyzer offering 300kHz–20GHz bandwidth and traceable phase response," in *IEEE MTT-S Int. Microw. Symp. Dig.*, Long Beach, CA, USA, Jun. 2005, p. 4.
- [12] W. Van Moer and Y. Rolain, "A large-signal network analyzer: Why is it needed?" *IEEE Microw. Mag.*, vol. 7, no. 6, pp. 46–62, Nov. 2006.
- [13] P. S. Blockley, J. B. Scott, D. Gunyan, and A. E. Parker, "The random component of mixer-based nonlinear vector network analyzer measurement uncertainty," *IEEE Trans. Microw. Theory Techn.*, vol. 55, no. 10, pp. 2231–2239, Oct. 2007.
- [14] M. Lin and Y. Zhang, "Covariance-matrix-based uncertainty analysis for NVNA measurements," *IEEE Trans. Instrum. Meas.*, vol. 61, no. 1, pp. 93–102, Jan. 2012.
- [15] G. Avolio, A. Raffo, J. Jargon, P. D. Hale, D. M. M.-P. Schreurs, and D. F. Williams, "Evaluation of uncertainty in temporal waveforms of microwave transistors," *IEEE Trans. Microw. Theory Techn.*, vol. 63, no. 7, pp. 2353–2363, Jul. 2015.
- [16] D. F. Williams and A. Lewandowski. (2011). NIST Microwave Uncertainty Framework. National Institute of Standards and Technology. [Online]. Available: <http://www.nist.gov/ct/rf-technology/relatedsoftware.cfm>

- [17] D. E. Root, J. Verspecht, J. Horn, and M. Marcu, *X-Parameters*. Cambridge, U.K.: Cambridge Univ. Press, 2013.
- [18] Network Measurement and Description Group (NMDG). (2009). *S-Functions, Measure, Model, Simulate, an Application in Integrated Component Characterization Environment*. [Online]. Available: <http://www.nmdg.be/newsletters/attach/SFunctions.pdf>
- [19] H. Qi, J. Benedikt, and P. J. Tasker, "Nonlinear data utilization: From direct data lookup to behavioral modeling," *IEEE Trans. Microw. Theory Techn.*, vol. 57, no. 6, pp. 1425–1432, Jun. 2009.
- [20] J. Verspecht, D. F. Williams, D. Schreurs, K. A. Remley, and M. D. McKinley, "Linearization of large-signal scattering functions," *IEEE Trans. Microw. Theory Techn.*, vol. 53, no. 4, pp. 1369–1376, Apr. 2005.
- [21] Analog Devices. *HMC342LC4 Datasheet*. Accessed: Nov. 20, 2018. [Online]. Available: <http://www.analog.com/media/en/technical-documentation/data-sheets/hmc342.pdf>
- [22] BIPM, IEC, IFCC, ILAC, ISO, IUPAC, IUPAP and OIML, *Guide to the Expression of Uncertainty in Measurement*, document JCGM 101:2008, Propagation of Distributions Using a Monte Carlo Method, ISO, Geneva, Switzerland, 2008. [Online]. Available: [http://www.bipm.org/utis/common/documents/jcgm/JCGM\\_101\\_2008\\_E.pdf](http://www.bipm.org/utis/common/documents/jcgm/JCGM_101_2008_E.pdf)
- [23] BIPM, IEC, IFCC, ILAC, ISO, IUPAC, IUPAP and OIML, *Guide to the Expression of Uncertainty in Measurement*, document JCGM 100:2008, ISO, Geneva, Switzerland, 2008. [Online]. Available: [http://www.bipm.org/utis/common/documents/jcgm/JCGM\\_100\\_2008\\_E.pdf](http://www.bipm.org/utis/common/documents/jcgm/JCGM_100_2008_E.pdf)
- [24] G. F. Engen and C. A. Hoer, "Thru-reflect-line: An improved technique for calibrating the dual six-port automatic network analyzer," *IEEE Trans. Microw. Theory Techn.*, vol. MTT-27, no. 12, pp. 987–993, Dec. 1979.
- [25] R. B. Marks, "A multiline method of network analyzer calibration," *IEEE Trans. Microw. Theory Techn.*, vol. 39, no. 7, pp. 1205–1215, Jul. 1991.
- [26] *Fundamentals of RF and Microwave Power Measurements (Part 3)*, Keysight Technologies, Santa Rosa, CA, USA, 2014.
- [27] Keysight Technologies. *U9391C/F/G Datasheet*. Accessed: Nov. 20, 2018. [Online]. Available: <http://literature.cdn.keysight.com/litweb/pdf/U9391-90001.pdf>
- [28] H. C. Reader, D. F. Williams, P. D. Hale, and T. S. Clement, "Comb-generator characterization," *IEEE Trans. Microw. Theory Techn.*, vol. 56, no. 2, pp. 515–521, Feb. 2008.
- [29] P. D. Hale *et al.*, "Traceable waveform calibration with a covariance-based uncertainty analysis," *IEEE Trans. Instrum. Meas.*, vol. 58, no. 10, pp. 3554–3568, Oct. 2009.



**Laurence T. Stant** (S'15) received the B.Sc. degree in physics (Hons.) from the University of Surrey, Guildford, U.K., in 2014, where he is currently pursuing the Ph.D. degree in microwave engineering.

He is currently an RF Engineer with Diamond Light Source, Oxfordshire, U.K. He is with the Electromagnetics Group, National Physical Laboratory, Teddington, U.K. His current research interests include measurement uncertainty and nonlinear microwave metrology.



**Martin J. Salter** (M'05) received the B.Sc. degree in physics from the University of Manchester, Manchester, U.K., in 1986, and the M.Sc. degree in microwave engineering from University College London, London, U.K., in 1991.

In 1986, he joined the Electromagnetics Group, National Physical Laboratory, Teddington, U.K. He is a member of the Nonlinear Microwave Measurement and Modelling Laboratories, a joint University of Surrey, Guildford, U.K./National Physical Laboratory. In 2015, he was a Visiting Researcher with

the Korean Research Institute of Standards and Science, Daejeon, South Korea. His current research interests include high-frequency electromagnetic measurements.



**Nick M. Ridler** (SM'06–F'14) received the B.Sc. degree from the Kings College, University of London, London, U.K., in 1981.

He has been involved in industrial, government, and academic research establishments. He is currently the Science Leader of electromagnetics and a Principal Research Scientist with the National Physical Laboratory, Teddington, U.K. He is also the Nonexecutive Director of LA Techniques Ltd., Surbiton, U.K., and a Visiting Professor with the Institute of Microwaves and Photonics, The University of Leeds, Leeds, U.K., Department of Electrical Engineering and Electronics, University of Liverpool, Liverpool, U.K., and the Advanced Technology Institute, University of Surrey, Guildford, U.K. His current research interests include high-frequency precision electromagnetic measurement (1 kHz–1 THz).

Mr. Ridler is a Fellow of the Institution of Engineering and Technology and the Institute of Physics. He is the Chair of the IEEE MTT Society's Standards Coordinating Committee, the Past Chair of the IEEE MTT Society's Microwave Measurements Technical Committee, and the Past President of the Automatic RF Techniques Group. He was a recipient of the Fellowship in Nonlinear Microwave Measurement with the Advanced Technology Institute, University of Surrey.



**Dylan F. Williams** (M'80–SM'90–F'02) received the Ph.D. degree in electrical engineering from the University of California at Berkeley, Berkeley, CA, USA, in 1986.

In 1989, he joined the Electromagnetic Fields Division, National Institute of Standards and Technology, Boulder, CO, USA, where he was involved in the development of electrical waveform and microwave metrology. He has authored or co-authored over 100 technical papers.

Dr. Williams was the Editor-In-Chief of the IEEE TRANSACTIONS ON MICROWAVE THEORY AND TECHNIQUES from 2006 to 2010. He has served as the Executive Editor of the IEEE TRANSACTIONS ON TERAHERTZ SCIENCE AND TECHNOLOGY. He was a recipient of the Department of Commerce Bronze and Silver Medals, the Astin Measurement Science Award, two Electrical Engineering Laboratory Outstanding Paper Awards, three Automatic RF Techniques Group Best Paper Awards, the ARFTG Automated Measurements Technology Award, the IEEE Morris E. Leeds Award, the European Microwave Prize, and the 2013 IEEE Joseph F. Keithley Award.



**Peter H. Aaen** (S'93–M'97–SM'09) received the B.A.Sc. degree in engineering science and M.A.Sc. degree in electrical engineering from the University of Toronto, Toronto, ON, Canada, in 1995 and 1997, respectively, and the Ph.D. degree in electrical engineering from Arizona State University, Tempe, AZ, USA, in 2005, respectively.

He was the Manager of the RF Modeling and Measurement Technology Team, RF Division, Freescale Semiconductor, Inc., Tempe, AZ, USA. In 1997, he was with Motorola Inc. Semiconductor Product Sector. In 2013, he joined the Faculty of Engineering and Physical Sciences, University of Surrey, Guildford, U.K., where he is currently a Reader in microwave semiconductor device modeling. He is also the Director of the Nonlinear Microwave Measurement and Modeling Laboratories, a joint University of Surrey/National Physical Laboratory, Teddington, U.K., and the Director of the National Physical Laboratory. He co-authored the *Modeling and Characterization of RF and Microwave Power FETs* (Cambridge Univ. Press, 2007).